Differential Effects of Alcohols on Conformational Switchovers in α-Helical and β-Sheet Protein Models†

Michael Perham,‡ Jue Liao,# and Pernilla Wittung-Stafshede*,‡,#,§

Department of Chemistry, Department of Biochemistry and Cell Biology, and Keck Center for Structural Computational Biology, Rice University, 6100 Main Street, Houston, Texas 77251

Received March 8, 2006; Revised Manuscript Received April 28, 2006

ABSTRACT: Organic solvents may induce non-native structures of proteins that mimic folding intermediates and/or conformations that occur in proximity to biological membranes. Here we systematically investigate the effects of simple (i.e., MeOH and EtOH) and fluorinated (i.e., trifluoroethanol, TFE) alcohols on the secondary structure and thermodynamic stability of two complementary model proteins using a combination of circular dichroism, fluorescence, and Fourier transform infrared (FTIR) detection methods. The selected proteins are α-helical *Borrelia burgdorferi* VlsE and β-sheet human mitochondrial co-chaperonin protein 10 (cpn10). We find that switches between VlsE's native and non-native superhelical and β-sheet structures readily occur (pH 7, 20 °C). The pathway depends on the alcohol: addition of MeOH induces a transition to a superhelical structure that is followed by conversion to β-structure, whereas EtOH only unfolds the protein. TFE unfolds VlsE at low percentages but promotes the formation of a superhelical state upon further additions. For cpn10, both MeOH and TFE additions govern initial unfolding; however, further additions of MeOH result in the formation of a non-native β-structure, whereas subsequent additions of TFE induce a superhelical structure. EtOH additions promptly unfold and precipitate cpn10. Both VlsE's and cpn10's non-native structures exhibit high stability toward chemical and thermal perturbations. This study demonstrates that in response to different alcohols, polypeptides can readily adopt both α- and β-enriched conformations. The biological significance of these findings is discussed.

The mechanism by which an unfolded polypeptide folds efficiently and rapidly into a unique three-dimensional (3D) structure from a very large conformational space available to it is a central problem in structural biology. It is clear that the folding of many proteins is guided by a limited number of partially folded intermediates on rather smooth and funnel-shaped free-energy landscapes (*1*−*9*). Information on properties of non-native states of proteins may thus provide insights into fundamental issues such as relationships between amino acid sequence and 3D structure, mechanisms of folding pathways, protein stability and turnover in the cells, and transport of proteins across membranes. In contrast to the large amount of structural, functional, and thermodynamic data existing on folded forms of proteins, there are only a limited number of biophysical/structural studies on non-native states of proteins. One of the most studied cosolvents in vitro that modifies protein structures is alcohol (*10*−*15*). Not only may alcohols induce non-native states in proteins that are of general biological relevance (*16*), alcohols are also of particular interest because of the similarity between these conditions and those near or in cellular membranes (*16*). Although most proteins are soluble, many require transport across membranes to reach their cellular destinations or function in proximity to membranes. In vitro studies involving alcohols may therefore report on transient or long-lived protein conformations that (a) partake in normal protein folding, transport, and degradation pathways in living cells and/or (b) are adopted in response to various stress or disease conditions.

Alcohols are known to stabilize helical secondary structures but destabilize tertiary structures of folded proteins. These mixed effects on polypeptides may cause the formation of non-native conformations. For example, additions of alcohols have been reported to induce partially folded states with high helical content in vitro of ribonuclease A, ubiquitin, cytochrome *c*, myoglobin, and lysozyme (*10*−*15*). The efficiencies of the destabilization of tertiary structure and stabilization of helical secondary structure vary significantly depending on the kind of alcohol used. The order of effectiveness toward destabilization of protein tertiary structures is believed to be trifluoroethanol (TFE)[1] > propanol > ethanol (EtOH) > methanol (MeOH) (*17*, *18*). The order appears the same for effectiveness toward stabilization of helical structures. In contrast to the concept that all alcohols are strong helix inducers in globular proteins, it was recently shown that non-fluorinated alcohols induced a switch from α-helix to β-sheet structure in the cysteine protease ervatamin C, which has a native α/β fold (*19*). Except for the ervatamin

† Support for this project was provided by grants from NIH (GM059663) and the Robert A. Welch Foundation (C-1588).

* Corresponding author. Phone: 713-348-4076; fax: 713-348-5154; e-mail, pernilla@rice.edu.

‡ Department of Chemistry.

Department of Biochemistry and Cell Biology.

§ Keck Center for Structural Computational Biology.

[1] Abbreviations: CD, circular dichroism; TFE, trifluoroethanol; MeOH, methanol; EtOH, ethanol; VlsE, variable major protein-like sequence, expressed; cpn10, co-chaperonin protein 10; FTIR, Fourier transform infrared.

10.1021/bi060464v CCC: $33.50
Published on Web 06/01/2006

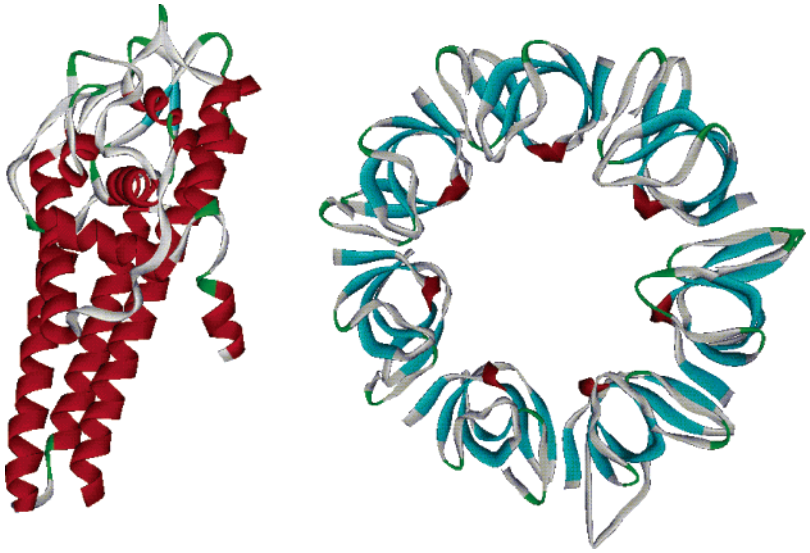

FIGURE 1: Structural models of the two proteins, VlsE (left; PDB file 1LW8) and cpn10 (right; structure reported in ref *30*). In both, α-helices are red, *β*-sheets are blue, *β*-hairpins are green, and random-coils are gray.

C study, the possibility of alcohol-induced *β*-structures in globular proteins has received little attention.

In a quest to systematically probe the effects of alcohols, we here report a spectroscopic study of the consequences of simple (i.e., MeOH and EtOH) and fluorinated (i.e., TFE) alcohols on the structure and stability of two model proteins (Figure 1). The models were selected to include proteins with contrasting secondary structures: *Borrelia burgdorferi* VlsE is a large (341 residues) single-domain protein with mostly α-helical structure (*20*−*24*), and human mitochondrial co-chaperonin protein 10 (cpn10) is a heptameric protein (100 residues per monomer) with seven *β*-barrels linked via interprotein *β*-strand pairing (*25*−*30*). Both proteins have been characterized previously in our laboratory in terms of their chemical and thermal unfolding behaviors (*20*, *21*, *31*−*36*). They unfold in apparent two-state reactions upon chemical and thermal perturbations, and, in each case, unfolding is reversible. This background information makes the proteins excellent targets for the current study. Here we demonstrate that the three alcohols induce distinct conformational changes in the model proteins, separated by high energy barriers, which are not easily predicted from the chemistry of the alcohols. Since, regardless of the native fold, switches between α- and *β*-enriched structures readily occur, and at some conditions unfolded structures are favored, we conclude that alcohols should not be viewed as simple "helix inducers".

MATERIALS AND METHODS

Human Mitochondrial cpn10. Preparation of human mitochondrial cpn10 from recombinant *Escherichia coli* has been described previously (*30*, *37*). In this paper, all "cpn10" data imply a Leu11Gly variant of cpn10. This mutation does not perturb the native structure of cpn10 nor its co-chaperonin function (unpublished results). The variant was selected for this study because it unfolds in simple apparent two-state (folded heptamer-to-unfolded monomers) equilibrium reactions in both urea and GuHCl; this is in contrast to wild-type cpn10 that adopts an assembled unfolded state in urea (*33*, *34*). Protein concentration was determined from $\epsilon_{278} = 4200\ M^{-1}\ cm^{-1}$ (50 mM Tris-HCl, 135 mM NaCl, 6 M GuHCl) established by amino acid analysis. The QuickChange Site-Directed Mutagenesis kit (Stratagene) was used to construct Leu11Gly cpn10 as described in ref *34*. The mutation was confirmed by DNA sequencing. Protein expression was performed by the stimulation of T7/Lac expression using a pET24d (Novagen) construct by addition of 2 mM IPTG (Promega). Purification of cpn10 was carried out as previously described (*34*) with the following minor alterations: cells were broken by an Emulsiflex C-50 cell breaker, and DNA precipitation was performed prior to ammonium-sulfate precipitation.

VlsE. The cloning procedure of VlsE from *Borrelia burgdorferi* strain B31 into a T7/NT-TOPO vector which incorporates an N-terminal His-tag has been reported previously (*20*, *21*). For protein expression, transformed BL21-(DE3) pLysS cells were used, and protein expression was induced by the addition of 3 mM IPTG. The cells were harvested and resuspended in 20 mM phosphate (pH 7.4), containing 0.5 M NaCl and 10 mM imidazole. Cells were broken by an Emulsiflex C-50 cell breaker. Upon removing cell debris, the supernatant was injected into a $NiSO_4$ column (Amersham Pharmacia) connected to an FPLC chromatography system. His-tagged VlsE was eluted by the addition of 500 mM imidazole. Protein fractions were pooled and concentrated, followed by dialysis into 5 mM phosphate, pH 7.0. In this study, the His-tag was not removed. Earlier work showed that the presence of the His-Tag did not affect folded structure, thermodynamic stability, or unfolding/refolding processes of VlsE (*20*, *21*).

Spectroscopic Methods. Absorption spectra were measured on a Cary 50 spectrophotometer (1-cm cell). For far-UV circular dichroism (CD) measurements, AVIV-62 and JASCO-810 spectropolarimeters were used. In CD measurements (1-mm cell; spectra collected at 200−300 nm), the sample compartment was purged with nitrogen gas to avoid absorption by O_2. Fluorescence spectra (1-cm cell; excitation at 280 nm and emission spectra collected at 300−400 nm) were collected on a Varian Eclipse fluorometer. All experiments were performed at 20 °C in 5 mM phosphate buffer, pH 7, unless otherwise stated. For Fourier transform infrared (FTIR) experiments, proteins were prepared in 99.9% D_2O

(Cambridge Isotope Laboratories) and 99.5% MeOD (Fisher Scientific) to the specified ratio and a final protein concentration of 1 mM. Samples were incubated for 1 h to allow exchange of exposed H for ^{2}H. Samples were loaded onto a BioTools CaF_2 cell, and spectra were collected on a Nicolet Nexus FTIR spectrometer. The spectrometer was purged for 12 h with N_2 prior to collecting spectra to avoid water vapor interference, and the detector was cooled with liquid N_2. Spectra were analyzed on OMNIC 7.1a software from Thermo Electron Corporation.

Alcohol-Induced Perturbations. MeOH, EtOH, and TFE stocks were from Fischer Scientific, Aaper, and Sigma, respectively. Samples for VlsE and cpn10 equilibrium-titration experiments were prepared by mixing various alcohol-to-buffer volume-to-volume (v/v) percentages, ranging from 0 to 90%, with fixed protein concentrations (ranging from 10 to 100 μM). All samples were incubated for at least 2 h before measurements. In all spectroscopic experiments, appropriate background signals of alcohol/buffer mixtures without protein were subtracted. As TFE can quench tryptophan emission (*38*), the tyrosine emission data for both proteins were carefully inspected for organic solvent effects. All protein samples were also monitored for precipitation before and after measurements. All alcohol percentages are reported as volume-to-volume. When appropriate, two-state equations were used to fit the data points in the transitions. All titration experiments were performed at least in triplicate.

Thermal and Chemical-Denaturant Perturbations. Thermal unfolding reactions of cpn10 (30 μM) in various percentages of MeOH were monitored by both far-UV CD and fluorescence. Samples were heated from 20 to 90 °C with a scan rate of 2 °C/min. Pre- and postheating spectra were collected. Thermal unfolding of VlsE (30 μM) in 28% MeOH was monitored by far-UV CD and fluorescence, with similar settings as for cpn10. Chemical denaturant urea (ICN Biochemicals) was of highest purity and prepared immediately before use. Unfolding of VlsE as a function of urea concentration was probed by CD and fluorescence detections with and without the presence of 25% MeOH. Samples were incubated for 1 h prior to measurements. Neither protein-concentration dependence nor time dependence was observed in these experiments. The urea-induced transitions were reversible and fitted with two-state equations to obtain $\Delta G_U(H_2O)$ and ΔG_U(25% MeOH). Chemical-denaturant experiments with cpn10 in the presence of high percentages of MeOH were hampered by protein aggregation.

The intrinsic secondary-structure contents of VlsE and cpn10 were predicted based on their amino acid sequences using several secondary-structure prediction programs found on the Expasy web server (http://www.expasy.org), i.e., NPS@GOR4, NPS@HNN, PSIPRED, PROFsec, PHDsec, and PORTER. The results of these predictions for VlsE are 56 ± 10% α-helix, 0 to 10% β-sheet and the rest, random coil. For cpn10, the predictions suggest 12 ± 12% α-helix, 45 ± 10% β-structure, and the rest, random coil.

RESULTS

Alcohol-Induced Non-Native Structures of α-Helical VlsE. VlsE is largely α-helical with a few regions of β-strands and several loops adopting random-coil structures (Figure 1), as determined by analysis of the far-UV CD spectrum and via the crystal structure (*20*, *22*). Urea- and GuHCl-induced equilibrium unfolding reactions of VlsE occur in simple two-state processes corresponding to a low thermodynamic stability (relative to the chemically denatured state) for a protein of this size (*20*, *21*). Fluorescence and far-UV CD have been used to monitor VlsE unfolding (*20*, *21*): both the tyrosine fluorescence centered at 308 nm and the negative CD signal around 220 nm decrease in magnitude upon chemical denaturation. These spectroscopic changes are expected upon adopting a random-coil structure with solvent-exposed tyrosines.

We find that additions of MeOH to VlsE result in a two-step reaction (pH 7, 20 °C). Between 0 and 30% MeOH, there is a first conversion of native VlsE to a state with increased negative far-UV CD intensity, still retaining minima at 208 and 222 nm characteristic of α-helices, and increased tyrosine emission (Figure 2A,B). These features imply a superhelical structure for the VlsE polypeptide. Further additions of MeOH result in a second highly cooperative transition that has a midpoint at 40% MeOH. The new state populated above 40% MeOH is characterized by less fluorescence and a decreased magnitude of negative far-UV CD. Moreover, the shape of the CD spectrum now has only one negative minimum at 215−220 nm (Figure 2B). This suggests the formation of a β-strand structure with solvent-exposed tyrosines. Both MeOH-induced transitions in VlsE are fully reversible. Fitting the second transition to a two-state equation results in an estimate of the free-energy difference between the superhelical and β-enriched states of ∼50 kJ/mol (pH 7, 20 °C), see Table 1.

In contrast to the MeOH data, additions of EtOH result in VlsE unfolding in a simple reversible, two-state reaction with a midpoint of about 40% EtOH (Figure 2C,D). Fluorescence and CD signals of VlsE in, or above, 40% EtOH match the corresponding signals found for VlsE in high concentrations of urea and GuHCl. The estimated free energy of unfolding derived from a two-state fit to the EtOH-induced transition is ∼16 kJ/mol (pH 7, 20 °C; Table 1); this value is in good agreement with the value derived from chemical-denaturant experiments (*20*, *21*), in support of an unfolding process.

In contrast to the nonfluorinated alcohols, TFE additions, between 0 and 20%, to VlsE result in prompt protein unfolding, as concluded from the decreases in fluorescence and negative far-UV CD signals (Figure 2E,F). Further additions of TFE induce an abrupt switch (around 30−40% TFE) to a state characterized by high fluorescence intensity and large negative CD magnitude. The CD spectra at these conditions have strong minima at 208 and 222 nm, indicating a large content of α-helices as would be the case for a superhelical structure. Fitting of this transition to determine a free-energy difference between the unfolded and the superhelical states could not be performed due to partial precipitation of protein samples within the transition region.

Alcohol-Induced Non-Native States in β-Sheet cpn10. cpn10 is an oligomeric protein of seven identical polypeptides that each forms an irregular β-barrel (Figure 1). The monomers are connected in a ring-shaped molecule via interprotein β-strand pairings (*29*, *30*). The far-UV CD signal of native cpn10 has a positive peak around 230 nm from tyrosine tertiary interactions and negative peak at 220 nm from the β-sheets. GuHCl-induced equilibrium unfolding of cpn10, as monitored by far-UV CD, cross-linking and

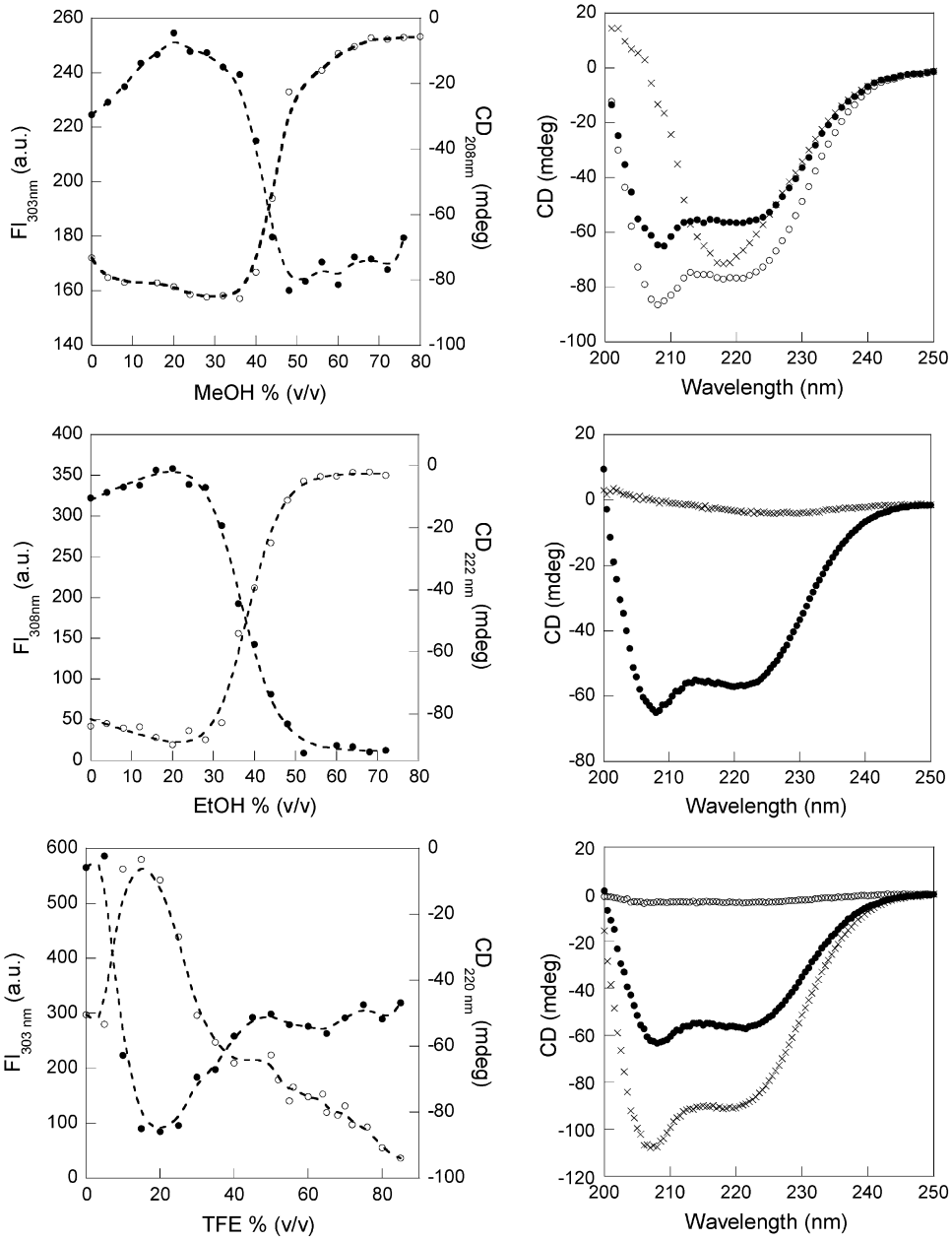

FIGURE 2: Left: Alcohol-induced changes in VlsE as monitored by far-UV CD (at 222 nm; open circles) and fluorescence at 303 nm (excitation at 280 nm; filled circles) as a function alcohol percent (from top to bottom; MeOH, EtOH, and TFE data). The dashed lines are included to guide the eye along each transition; they are mostly smooth fits, and only in a few cases were two-state fits employed (see text). Right: Far-UV CD spectra of VlsE in the presence of different alcohol percentages. Native VlsE in buffer is shown by filled circles in all three panels. Top panel: open circles, 27% MeOH; crosses, 73% MeOH. Middle panel: crosses, 70% EtOH. Bottom panel: open circles, 24% TFE; crosses, 80% TFE.

tyrosine fluorescence, is an apparent two-state reaction in which polypeptide unfolding and protein dissociation is coupled. The free-energy of unfolding/dissociation is about 30 kJ/mol monomer (pH 7, 20 °C) (*33*). This value is to ~90% contributed by the interface interactions; cpn10 monomers can be folded in isolation but are marginally stable (*35*).

Addition of MeOH to cpn10 results in a sharp switch, around 45% MeOH, to a state that has less CD intensities at 220 and 230 nm in combination with decreased tyrosine emission. These changes indicate that cpn10 is adopting an unfolded-like structure (Figure 3A,B). Further additions of MeOH lead to cooperative formation of a structure that has high β-strand content (i.e., large negative CD signal with minimum at 215 nm and high fluorescence) at around 75% MeOH. Assuming a two-state unfolded-to-β process, the corresponding free-energy is estimated to 31 ± 3 kJ/mol (buffer, pH 7, 20 °C).

Upon EtOH additions to cpn10, the protein unfolds, in parallel with immediate precipitation, at 35 and higher percentages. This is clear from both the far-UV CD and the fluorescence data (Figure 3C,D). In addition, the solutions become visually cloudy.

Like the MeOH perturbation of cpn10, TFE additions to cpn10 result in initial unfolding of the protein according to CD- and fluorescence-signal changes (transition midpoint at ~15% TFE). In contrast to the reaction in MeOH, further additions of TFE lead to the appearance of a very strong negative CD signal with minima at 208 and 222 nm and increased tyrosine emission (Figure 3E,F). The transition

Table 1: Summary of Alcohol-Induced Effects on VlsE and cpn10 Induced by MeOH, EtOH, and TFE Solvents[a]

	MeOH			EtOH			TFE		
protein	change	midpoint	$\Delta G(H_2O)$	change	midpoint	$\Delta G(H_2O)$	change	midpoint	$\Delta G(H_2O)$
VlsE	$\alpha_N \rightarrow \alpha$	15%	n.d.	$\alpha_N \rightarrow$ unf	40%	16 ± 2 kJ/mol[e]	$\alpha_N \rightarrow$ unf	7%	n.d.
	$\alpha \rightarrow \beta$	43%	51 ± 6 kJ/mol[e]				unf $\rightarrow \alpha$	35%	n.d.
urea 0% MeOH	$\alpha_N \rightarrow$ unf	1.2 M	13 ± 2 kJ/mol[e]						
urea 25% MeOH	$\alpha \rightarrow$ unf	2.0 M	19 ± 2 kJ/mol[e]						
cpn10	$\beta_N \rightarrow$ unf	45%	n.d.	$\beta_N \rightarrow$ unf	35%	n.d.	$\beta_N \rightarrow$ unf	15%	n.d.
	unf $\rightarrow \beta$	75%	31 ± 3 kJ/mol[c]				unf $\rightarrow \alpha$	25%	25 ± 4 kJ/mol[d]
0% MeOH	$\beta_N \rightarrow$ unf	65 ± 2 °C	n.d.						
20% MeOH	$\beta_N \rightarrow$ unf	48 ± 2 °C	n.d.						
50% MeOH	unf $\rightarrow \alpha$	60 ± 3 °C	n.d.						
80% MeOH	$\beta \rightarrow \alpha$	75 ± 3 °C	n.d.						

[a] In each case, the structural change observed, the transition midpoint and the corresponding free energy (if calculated) are reported. The alcohol percentages are reported as volume-to-volume percent. All results refer to pH 7 and 20 °C conditions, except for the thermal data in MeOH for cpn10. Both far-UV CD and fluorescence detection methods were used in the experiments. [b] n.d. not determined. [c] Fluorescence data used for fit. [d] CD at 227 nm data used for fit. [e] CD at 222 nm and fluorescence data used for fits.

midpoint for this process is found at ~25% TFE and corresponds to a free-energy difference of ~25 kJ/mol (in buffer, pH 7, 20 °C). The spectroscopic signals are compatible with the formation of a superhelical state of the cpn10 polypeptide at high TFE concentrations. The unfolded state of cpn10 adopted at intermediate TFE concentrations was prone to precipitation upon extended room-temperature incubation.

Structural Analysis of Non-Native States by FTIR. FTIR spectroscopy was used to gain further insight into the secondary-structure content of the MeOH-induced non-native states. FTIR spectra in the amide I region (1600−1700 cm^{-1}; reporting on secondary structures (*39*−*41*)) were collected on deuterated MeOH/buffer solutions of fixed VlsE concentrations but varied MeOH percentages. As expected, the FTIR spectrum of native VlsE in buffer (pH 7, 20 °C) is dominated by a strong absorbance at 1654 cm^{-1} corresponding to α-helices (*39*−*41*). In the presence of 28% MeOH, this band is intensified without any band-shift, indicating the formation of additional α-helical secondary structure. Spectra at higher MeOH amounts (i.e., 41 and 70% MeOH) reveal decreased absorbance at 1654 cm^{-1} in parallel with new bands appearing at 1616 and 1683 cm^{-1} (Figure 4). These two latter wavenumbers are indicative of β-strand-containing structures (*39*−*41*). Notably, identical FTIR band changes as observed here for VlsE were reported for the helical tetramerization domain of p53 upon high-temperature incubation. In that case, intermolecular β-strand formation was concluded (*42*). The FTIR results on VlsE reinforce that at intermediate concentrations of MeOH (i.e., around 30%) VlsE adopts a superhelical structure that is converted to a β-enriched structure upon further additions of MeOH (i.e., above 45%). FTIR experiments on cpn10 in MeOH were hampered by precipitation at the high protein concentrations required.

Thermal and Chemical-Denaturant Perturbation of Non-Native States. To assess the relative stability of the non-native states observed in MeOH, chemical and thermal experiments were performed with VlsE and cpn10 at different MeOH conditions. Urea-induced equilibrium unfolding of native VlsE exhibits a transition midpoint at ~1.2 M urea (pH 7, 20 °C) that corresponds to a free energy of unfolding of ~13 kJ/mol (Table 1). An identical unfolding experiment of VlsE in its superhelical state (i.e., VlsE in the presence of 25% MeOH) reveals that the transition remains cooperative and shifts to higher urea concentrations: the midpoint is now found at 2.0 M urea (Figure 5A), regardless of the detection method, and the free energy for the transition increases to ~19 kJ/mol (Table 1). In contrast, thermal unfolding of VlsE in the presence of 28% MeOH (i.e., in the superhelical state) results in a transition that is shifted to a lower thermal midpoint (T_m) as compared to that observed for native VlsE in buffer (T_m values of 44 ± 3 and 56 ± 3 °C, respectively; data not shown). Like the urea data in MeOH, the thermal-unfolding transitions of VlsE in the presence of MeOH are identical regardless of far-UV CD or fluorescence detection, indicating the absence of populated intermediates. Since the superhelical state of VlsE has a higher stability than native VlsE toward chemical but not thermal perturbation, it implies that these two structural states of VlsE have different entropic and enthalpic sensitivities.

Chemical-denaturant (urea or GuHCl) induced unfolding of cpn10 in the presence of MeOH percentages sufficient to induce the nonnative β-structure (i.e., >80% MeOH) could not be carried out due to precipitation. Nonetheless, thermal experiments could be executed with cpn10 in the presence of different MeOH percentages. Equilibrium-thermal perturbation of native cpn10 is a reversible apparent two-state process (*33*). Because cpn10 is a heptamer and thermal perturbation results in unfolded monomers, the midpoints exhibit protein-concentration dependence. Therefore, the thermal data reported here are all for samples with a cpn10 concentration of 30 μM. Also in the presence of MeOH are single, apparent two-state transitions observed. CD and fluorescence detection methods give identical results at each condition. The T_m values are 65, 48, 60, and 75 °C in buffer, 20, 50, and 80% MeOH, respectively (Figure 5B; Table 1). These results show that the native state of cpn10 is somewhat destabilized by the presence of low amounts of MeOH (i.e., lower T_m in 20% MeOH than in buffer). Furthermore, in 50 and 80% MeOH, heating results in the formation of a superhelical state at high temperatures (inset, Figure 5B), regardless of whether the starting structure is random-coil (i.e., in 50% MeOH) or non-native β-strands (i.e., in 80% MeOH). Finally, it emerges that the non-native β-structure is more resistant than the native state of cpn10 toward thermal perturbation (i.e., T_m values of 75 and 65 °C for cpn10 in 80 and 0% MeOH, respectively).

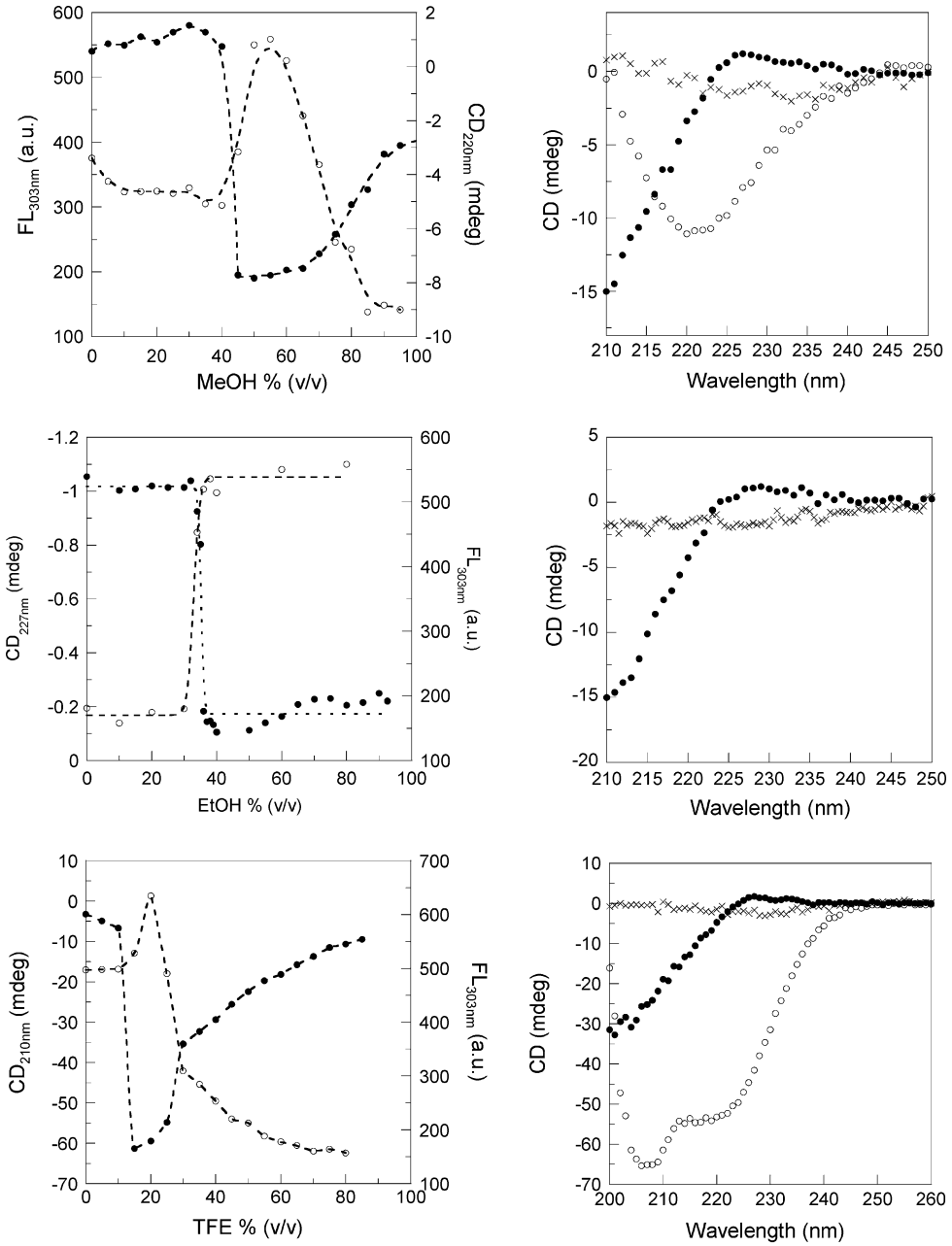

FIGURE 3: Left: Alcohol-induced changes in cpn10 as monitored by far-UV CD (at 220, 227, or 210 nm, as indicated on *y*-axes; open circles) and fluorescence at 303 nm (excitation at 280 nm; filled circles) as a function alcohol percent (from top to bottom; MeOH, EtOH, and TFE data). The dashed lines are included to guide the eye along each transition; they are mostly smooth fits, and only in a few cases were two-state fits employed (see text). Right: Far-UV CD spectra of cpn10 in the presence of different alcohol percentages. Native cpn10 in buffer is shown by filled circles in all three panels. Top panel: open circles, 80% MeOH; crosses, 55% MeOH. Middle panel: crosses, 40% EtOH. Bottom panel: open circles, 75% TFE; crosses, 20% TFE.

DISCUSSION

Perturbations of Proteins by Alcohols. Water/alcohol mixtures have been suggested as useful model systems for studies of the action on protein structures of the local decrease in dielectric constant near membrane surfaces. In addition, for several proteins, alcohol-induced non-native states have been shown to have properties identical to those of real folding intermediates (*10*−*15*). Precisely how alcohols perturb protein structures is not known (*43*, *44*). The effects of alcohols have been attributed to ordering of solvent molecules, lowering the dielectric constant of the solvent, hydrophobic effects, changes in hydrogen bonding along the peptide chain, or some combination of these (*16*). Typically, alcohol-induced denaturation of globular proteins is accompanied by a characteristic increase in α-helical content. The existence of highly helical conformations and disrupted tertiary structures in alcohols has been reported for many proteins and is summarized in Table 2 (*10*−*15*, *17*, *18*). Although the size and overall shape of these states are not fully known, they have been proposed to have expanded and flexible nonglobular, rodlike chain conformations, in which the rods are usually helical (*10*−*15*).

Should Alcohols Really Be Considered "Helix Inducers"? Our findings challenge the concept of alcohols as simple helix inducers. Using two model proteins (Figure 1), we demonstrate by spectroscopic methods that non-fluorinated alcohols (e.g., MeOH and EtOH) can induce α-, *β*-, and unfolded structures, regardless of the protein's native fold

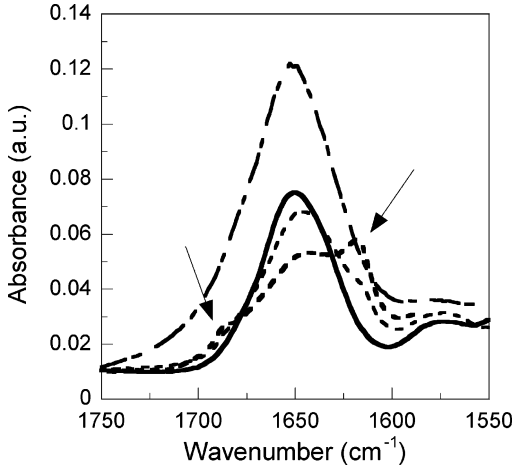

FIGURE 4: FTIR spectra in the amide I region of VlsE in 0% (solid thick line), 28% (thin long dashed line), 41% (thin dashed line) and 70% (thick dashed line) MeOH (pH 7, 20 °C). All samples were prepared in deuterated solvents with 1 mM VlsE. Arrows indicate the new bands that correspond to β-structures (see text).

(Figures 2−4). TFE, on the other hand, only induces unfolding or α-enriched structures in our model proteins (Table 1; Figure 6). It is worth mentioning that we make similar observations as those reported here for VlsE and cpn10 on another unrelated protein: the blue-copper protein *Pseudomonas aeruginosa* azurin. MeOH additions to the apo-form of azurin promote a superhelical state at intermediate MeOH percentages that converts to a non-native β-structure at higher MeOH percentages, whereas TFE induces only a superhelical state in this protein (J.L., P.W.S.; unpublished results).

We find that the non-native α- and β-enriched states of VlsE and cpn10 form in cooperative transitions; the thermodynamic estimates reveal that the apparent free energies involved in these reactions are high (Table 1). We note that these values must be viewed as approximations as they do not account for any interprotein interactions. Despite no detected precipitation, some interprotein associations cannot be excluded. Nonetheless, the intrinsic stability of the non-native superhelical and β-enriched states of VlsE and cpn10, respectively, is also clear from the chemical and thermal perturbation experiments in the presence of MeOH (Figure 5). Although no thermodynamic parameters have been reported previously for non-native states in organic solvents, higher stability toward thermal and chemical perturbations has been reported for a few proteins (e.g., ervatamin C and barstar) in the presence of alcohols (*19*, *45*). The presence of large energetic separations between the non-native conformations, and their apparent high stabilities, suggests that protein-folding free-energy landscapes include deep narrow minima, corresponding to distinct non-native structures, in addition to the funnel-shaped well that leads to the native fold.

What Is the Implication of the Alcohol-Induced α → β *Crossover?* To our knowledge, this is the first report of an all α-helical protein (i.e., VlsE) switching to a β-enriched structure in the presence of alcohol. Similar behavior has only been found for two other globular proteins and two random-coil structured polypeptides (Table 2). A switch from the native α/β structure of ervatamin C to a non-native β-sheet structure was found in the presence of non-fluorinated

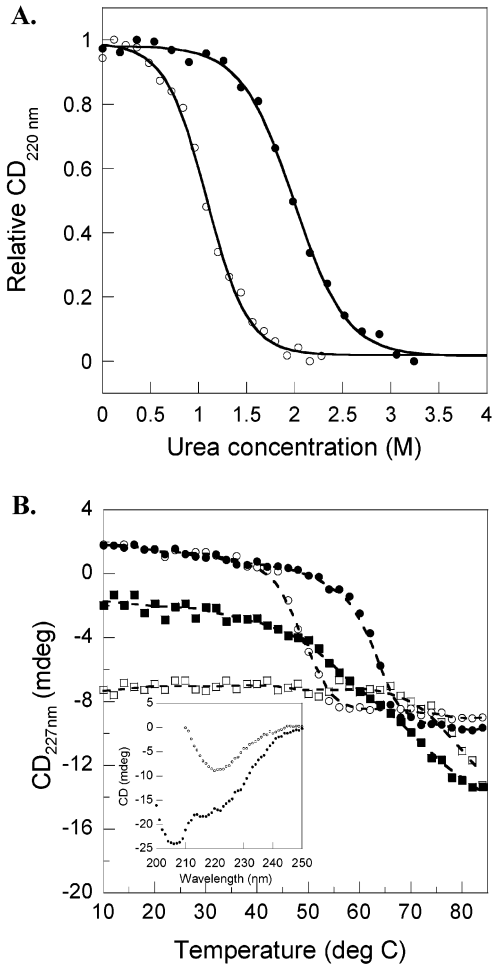

FIGURE 5: (A) Urea-induced equilibrium unfolding of VlsE in 0% (open circles) and 25% (filled circles) MeOH. The CD signals are scaled to the same total change for clarity. Solid lines are two-state fits to the data points (Table 1). (B) cpn10 thermal denaturation in the presence of various MeOH percentages. Filled circles, 0% MeOH; open circles, 20% MeOH; filled squares, 50% MeOH; open squares, 80% MeOH. The thermal midpoint for each condition is reported in Table 1. Inset: CD signal at 20 °C (open squares) and 80 °C (filled squares) for cpn10 in 80% MeOH, demonstrating the β-enriched starting structure at room-temperature and the superhelical structure adopted at high temperatures.

alcohols (*19*). In addition, β-sheet induction by MeOH was reported in muscle acetylphosphatase; however, the induced structure was considered to be partial formation of a native β-sheet (*46*). Furthermore, α-synuclein, which is a natively unfolded protein, adopted both α- and β-structures depending on the alcohol added (*47*). Such a dual behavior has also been demonstrated with poly-L-lysine, a polypeptide that is random-coil in buffer at pH 7. Addition of low concentrations of non-fluorinated alcohols to poly-L-lysine results in β-sheet formation, whereas high concentrations of these alcohols result in α-helical structures (*48*). The ability of polypeptides to adopt both α- and β-enriched conformations emphasizes the importance of evaluating the presence of non-native secondary structures in folding intermediates and folding-transition states. For example, β-lactoglobulin has been proposed to fold to its native β-sheet structure via a non-native α-helical intermediate (*49*). Notably, phi-value analysis of transition-state structures is often interpreted assuming only the presence of nativelike interactions (*50*−*54*).

Table 2: Summary of Alcohol-Induced Protein Changes Described in the Literature Resulting in α- and *β*-Enriched Structures[a]

alcohol-induced α-*structure*		
protein	native fold	alcohol[b]
α-synuclein	random	TFE, HFiP
ervatamin C	α/*β*	TFE
acylphosphatase	*β*	TFE
poly-L-lysine	random	high MeOH, EtOH, PrOH
cytochrome *c*	α	MeOH
myoglobin (apo)	α	MeOH
ribonuclease A	α/*β*	MeOH
ubiquitin	α/*β*	MeOH
lysozyme	α/*β*	DMSO, TFE, MEOH, EtOH
α-lactalbumin	α/*β*	MeOH
β-lactoglobulin	*β*	MeOH, EtOH, PrOH
subtilisin inhibitor	α/*β*	MeOH
apo-azurin[c]	*β*	MeOH, TFE
cpn10[d]	*β*	TFE
VlsE[d]	α	TFE

alcohol-induced *β*-*structure*		
protein	native fold	alcohol[b]
α-synuclein	random	MeOH, EtOH, PrOH
ervatamin C	α/*β*	MeOH, EtOH
acylphosphatase	*β*	MeOH, EtOH
poly-L-lysine	random	low MeOH, EtOH, ProOH
apo-azurin[c]	*β*	MeOH
cpn10[d]	*β*	MeOH
VlsE[d]	α	MeOH

[a]For each protein, the native fold as well as the alcohol used is provided. The conditions in each case may very, although most studies were performed at room temperature and neutral to acidic pH. [b] HFiP, hexafluoro propanol; PrOH, propanol; DMSO, dimethyl sulfoxide.[c] JL, PWS; unpublished results. [d] This study.

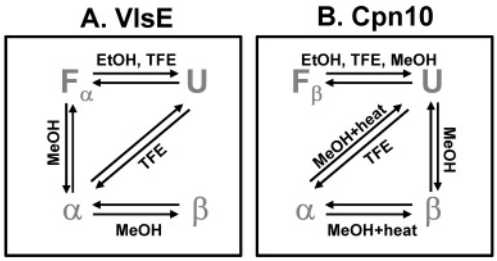

FIGURE 6: Schemes linking the folded (F) and unfolded (U; i.e., random-coil) states of VlsE (A) and cpn10 (B) with non-native superhelical (α) and *β*-enriched (*β*) structures. Arrows indicate the reactions that are observed in the presence of the different alcohols in vitro (Table 1). For both proteins, F-to-U transitions are observed in chemical denaturants and in EtOH. For VlsE (A), F-to-α followed by α-to-*β* transitions are observed in MeOH and F-to-U followed by U-to-α transitions in TFE. For cpn10 (B), F-to-U followed by U-to-*β* transitions are observed in MeOH and F-to-U followed by U-to-α transitions in TFE. In addition, upon heating of cpn10 in MeOH, *β*-to-α or U-to-α transitions can occur.

Can Our Observations Be Explained by Alcohol Chemistry? The effects of alcohols appear to be a combination of the hydrophobicity of the aliphatic chain and the hydrogen-bond donor ability of the hydroxyl group (*43*, *44*). The dielectric constants are ~78, 33, 28, and 25, for water, MeOH, TFE, and EtOH, respectively; the dipole moment is 2.52, 1.84, 1.70, 1.69 for TFE, water, MeOH, and EtOH, respectively. Whereas MeOH and EtOH are weaker acids than water, TFE is a stronger acid than water (*43*, *44*). EtOH has the lowest dielectric constant and, perhaps due to this high hydrophobicity, does not induce distinct non-native structures except for causing protein unfolding and precipitation. On the other hand, since TFE is most polar of the three solvents, its ability to displace water and act as a proton donor may explain why it so strongly favors α-helical structure formation in proteins (*16*). Indeed, several recent publications have shown that TFE preferentially binds to proteins (*55*−*57*). MeOH is less polar than TFE but not as hydrophobic as EtOH; apparently, these intermediate properties govern a range of structural effects in our systems. It has been proposed that MeOH and EtOH mimic the environment near membranes, whereas TFE mimics the environment in the membrane, i.e., the membrane-bound form of proteins (*47*). If true, our results in combination with the literature data (Table 2) suggest that membrane-bound forms (i.e., as modeled by TFE additions) of proteins will most often be α-helical, whereas proteins in proximity of membranes (i.e., as modeled by nonfluorinated alcohol additions) may adopt a range of non-native structures not easily predictable based on the protein's native fold.

Is There Biological Bearing of the Non-Native States Observed? First, VlsE is a surface protein, normally attached to the *Borrelia* spirochete surface via a lipid that is covalently linked to an N-terminal cysteine residue (*20*−*24*). Thus, VlsE is directly exposed to a membrane environment and packed tightly between other surface proteins. Conformational changes in VlsE may be a strategy by the spirochete to avoid rapid degradation in vivo and instead allow time for non-native states to be recognized by the host immune system. VlsE has many variable regions in its polypeptide, and thus host-generated antibodies are not deleterious to the spirochete. Interestingly, one VlsE peptide region that is hidden in the core of in native structure still triggers a strong immune response (*23*, *24*, *58*, *59*). In a diagnostic peptide-based test, it was shown that this peptide stretch binds antibodies better when the helical tendency of the peptide was improved (by alanine additions). This result directly supports that non-native helical structures of VlsE are populated in vivo. As for cpn10, it is a co-chaperonin and together with cpn60 interacts with substrate proteins that are either unfolded or partially folded (*25*−*30*). For this activity, it may be necessary for cpn10 to have a flexible structure that can encapsulate a variety of substrates. Moreover, non-native states of human cpn10 may be involved in its proposed activities during early pregnancy (*60*), in red blood cells that lack mitochondria (*61*), during carcinogenesis (*62*), and in human diseases related to protein misfolding (*63*). Notably, cpn10 from *E. coli*, GroES, has been shown to adopt *β*-sheet aggregates similar to amyloids at mild denaturing conditions in vitro (*64*). It was proposed that these structures are favored at conditions corresponding to non-native conformations.

CONCLUSIONS

We have systematically investigated the effects of simple (i.e., MeOH and EtOH) and fluorinated (i.e., TFE) alcohols on the structure and stability of α-helical *B. burgdorferi* VlsE and *β*-sheet human mitochondrial cpn10 using spectroscopic methods. We find that a natively α-helical protein can adopt non-native *β*-structures, and, on the other hand, natively *β*-sheet proteins can adopt α-helical structures. These conversions depend sensitively on the type and amount of alcohol added (Figure 6). Whereas TFE only causes protein unfolding or formation of superhelical structures, MeOH facilitates the formation of all of unfolded, superhelical as

well as β-enriched structures. Thus, alcohols are not simple "helix inducers" as is generally assumed. Our results show that the same polypeptide can adopt a variety of conformations in response to solvent changes; thus, the structures adopted by proteins near or in biological membranes, or during folding, may differ dramatically from those observed in dilute buffers and considered to be "native".

ACKNOWLEDGMENT

M.P. is supported by an NIH Biotech Fellowship (GM008326).

REFERENCES

1. Plaxco, K. W., Simons, K. T., and Baker, D. (1998) Contact order, transition state placement and the refolding rates of single domain proteins, *J. Mol. Biol. 277*, 985−994.
2. Plaxco, K. W., Simons, K. T., Ruczinski, I., and David, B. (2000) Topology, stability, sequence, and length: Defining the determinants of two-state protein folding kinetics, *Biochemistry 39*, 11177−11183.
3. Chavez, L. L., Onuchic, J. N., and Clementi, C. (2004) Quantifying the roughness on the free energy landscape: entropic bottlenecks and protein folding rates, *J. Am. Chem. Soc. 126*, 8426−8432.
4. Makarov, D. E., and Plaxco, K. W. (2003) The topomer search model: A simple, quantitative theory of two-state protein folding kinetics, *Protein Sci. 12*, 17−26.
5. Clementi, C., Jennings, P. A., and Onuchic, J. N. (2000) How native-state topology affects the folding of dihydrofolate reductase and interleukin-1beta, *Proc. Natl. Acad. Sci. U.S.A. 97*, 5871−5876.
6. Clementi, C., Jennings, P. A., and Onuchic, J. N. (2001) Prediction of folding mechanism for circular-permuted proteins, *J. Mol. Biol. 311*, 879−890.
7. Clementi, C., Nymeyer, H., and Onuchic, J. N. (2000) Topological and energetic factors: what determines the structural details of the transition state ensemble and "en-route" intermediates for protein folding? An investigation for small globular proteins, *J. Mol. Biol. 298*, 937−953.
8. Jackson, S. E. (1998) How do small single-domain proteins fold? *Fold Des. 3*, R81−R91.
9. Kamagata, K., Arai, M., and Kuwajima, K. (2004) Unification of the folding mechanisms of non-two-state and two-state proteins, *J. Mol. Biol. 339*, 951−965.
10. Bychkova, V. E., Dujsekina, A. E., Klenin, S. I., Tiktopulo, E. I., Uversky, V. N., and Ptitsyn, O. B. (1996) Molten globule-like state of cytochrome *c* under conditions simulating those near the membrane surface, *Biochemistry 35*, 6058−6063.
11. Kamatari, Y. O., Konno, T., Kataoka, M., and Akasaka, K. (1998) The methanol-induced transition and the expanded helical conformation in hen lysozyme, *Protein Sci. 7*, 681−688.
12. Kamatari, Y. O., Ohji, S., Konno, T., Seki, Y., Soda, K., Kataoka, M., and Akasaka, K. (1999) The compact and expanded denatured conformations of apomyoglobin in the methanol−water solvent, *Protein Sci 8*, 873−882.
13. Bhattacharjya, S., and Balaram, P. (1997) Effects of organic solvents on protein structures: observation of a structured helical core in hen egg-white lysozyme in aqueous dimethylsulfoxide, *Proteins 29*, 492−507.
14. Babu, K. R., and Douglas, D. J. (2000) Methanol-induced conformations of myoglobin at pH 4.0, *Biochemistry 39*, 14702−14710.
15. Dzwolak, W., Grudzielanek, S., Smirnovas, V., Ravindra, R., Nicolini, C., Jansen, R., Loksztejn, A., Porowski, S., and Winter, R. (2005) Ethanol-perturbed amyloidogenic self-assembly of insulin: looking for origins of amyloid strains, *Biochemistry 44*, 8948−8958.
16. Buck, M. (1998) Trifluoroethanol and colleagues: cosolvents come of age. Recent studies with peptides and proteins, *Q. Rev. Biophys. 31*, 297−355.
17. Herskovits, T. T., Gadegbeku, B., and Jaillet, H. (1970) On the structural stability and solvent denaturation of proteins. I. Denaturation by the alcohols and glycols, *J. Biol. Chem. 245*, 2588−2598.
18. Bianchi, E., Rampone, R., Tealdi, A., and Ciferri, A. (1970) The role of aliphatic alcohols on the stability of collagen and tropocollagen, *J. Biol. Chem. 245*, 3341−3345.
19. Sundd, M., Kundu, S., and Jagannadham, M. V. (2000) Alcohol-induced conformational transitions in ervatamin C. An alpha-helix to beta-sheet switchover, *J. Protein Chem. 19*, 169−176.
20. Jones, K., Guidry, J., and Wittung-Stafshede, P. (2001) Characterization of surface antigen from Lyme disease spirochete *Borrelia burgdorferi*, *Biochem. Biophys. Res. Commun. 289*, 389−394.
21. Jones, K., and Wittung-Stafshede, P. (2003) The largest protein observed to fold by two-state kinetic mechanism does not obey contact-order correlation, *J. Am. Chem. Soc. 125*, 9606−9607.
22. Eicken, C., Sharma, V., Klabunde, T., Lawrenz, M. B., Hardham, J. M., Norris, S. J., and Sacchettini, J. C. (2002) Crystal structure of Lyme disease variable surface antigen VlsE of *Borrelia burgdorferi*, *J. Biol. Chem. 277*, 21691−21696.
23. Liang, F. T., Alvarez, A. L., Gu, Y., Nowling, J. M., Ramamoorthy, R., and Philipp, M. T. (1999) An immunodominant conserved region within the variable domain of VlsE, the variable surface antigen of *Borrelia burgdorferi*, *J. Immunol. 163*, 5566−5573.
24. Liang, F. T., and Philipp, M. T. (1999) Analysis of antibody response to invariable regions of VlsE, the variable surface antigen of *Borrelia burgdorferi*, *Infect. Immun. 67*, 6702−6706.
25. Martin, J., Geromanos, S., Tempst, P., and Hartl, F. U. (1993) Identification of nucleotide-binding regions in the chaperonin proteins GroEL and GroES, *Nature 366*, 279−282.
26. Todd, M. J., Boudkin, O., Freire, E., and Lorimer, G. H. (1995) GroES and the chaperonin-assisted protein folding cycle: GroES has no affinity for nucleotides, *FEBS Lett 359*, 123−125.
27. Burston, S. G., Weissman, J. S., Farr, G. W., Fenton, W. A., and Horwich, A. L. (1996) Release of both native and non-native proteins from a cis-only GroEL ternary complex, *Nature 383*, 96−99.
28. Shtilerman, M., Lorimer, G. H., and Englander, S. W. (1999) Chaperonin function: folding by forced unfolding, *Science 284*, 822−825.
29. Hunt, J. F., Weaver, A. J., Landry, S. J., Gierasch, L., and Deisenhofer, J. (1996) The crystal structure of the GroES co-chaperonin at 2.8 Å resolution, *Nature 379*, 37−45.
30. Landry, S. J., Steede, N. K., and Maskos, K. (1997) Temperature dependence of backbone dynamics in loops of human mitochondrial heat shock protein 10, *Biochemistry 36*, 10975−10986.
31. Bascos, N., Guidry, J., and Wittung-Stafshede, P. (2004) Monomer topology defines folding speed of heptamer, *Protein Sci 13*, 1317−1321.
32. Brown, C., Liao, J., and Wittung-Stafshede, P. (2005) Interface mutation in heptameric co-chaperonin protein 10 destabilizes subunits but not interfaces, *Arch. Biochem. Biophys. 439*, 175−183.
33. Guidry, J. J., Moczygemba, C. K., Steede, N. K., Landry, S. J., and Wittung-Stafshede, P. (2000) Reversible denaturation of oligomeric human chaperonin 10: denatured state depends on chemical denaturant. *Protein Sci. 9*, 2109−2117.
34. Guidry, J. J., Shewmaker, F., Maskos, K., Landry, S., and Wittung-Stafshede, P. (2003) Probing the interface in a human co-chaperonin heptamer: residues disrupting oligomeric unfolded state identified, *BMC Biochem. 4*, 14.
35. Guidry, J. J., and Wittung-Stafshede, P. (2002) Low stability for monomeric human chaperonin protein 10: interprotein interactions contribute majority of oligomer stability, *Arch. Biochem. Biophys. 405*, 280−282.
36. Perham, M., Chen, M., Ma, J., and Wittung-Stafshede, P. (2005) Unfolding of heptameric co-chaperonin protein follows "fly casting" mechanism: observation of transient nonnative heptamer, *J. Am. Chem. Soc. 127*, 16402−16403.
37. Steede, N. K., Guidry, J. J., and Landry, S. J. (2000) Preparation of recombinant human Hsp10, *Methods Mol. Biol. 140*, 145−151.
38. Chen, Y., Liu., B., and Barkley, M. D. (1995) Trifluoroethanol quenches indole fluorescence by excited-state proton transfer, *J. Am. Chem. Soc. 117*, 5608−5609.
39. Fabian, H., Schultz, C., Naumann, D., Landt, O., Hahn, U., and Saenger, W. (1993) Secondary structure and temperature-induced unfolding and refolding of ribonuclease T1 in aqueous solution. A Fourier transform infrared spectroscopic study, *J. Mol. Biol. 232*, 967−981.

40. Byler, D. M., and Susi, H. (1986) Examination of the secondary structure of proteins by deconvolved FTIR spectra, *Biopolymers 25*, 469−487.
41. Cooper, E. A., and Knutson, K. (1995) Fourier transform infrared spectroscopy investigations of protein structure, *Pharm. Biotechnol. 7*, 101−143.
42. Lee, A. S., Galea, C., DiGiammarino, E. L., Jun, B., Murti, G., Ribeiro, R. C., Zambetti, G., Schultz, C. P., and Kriwacki, R. W. (2003) Reversible amyloid formation by the p53 tetramerization domain and a cancer-associated mutant, *J. Mol. Biol. 327*, 699−709.
43. Dwyer, D. S. (1999) Molecular simulation of the effects of alcohols on peptide structure, *Biopolymers 49*, 635−645.
44. Dwyer, D. S., and Bradley, R. J. (2000) Chemical properties of alcohols and their protein binding sites. *Cell. Mol. Life Sci. 57*, 265−275.
45. Khurana, R., and Udgaonkar, J. B. (1994) Equilibrium unfolding studies of barstar: evidence for an alternative conformation which resembles a molten globule, *Biochemistry 33*, 106−115.
46. Chiti, F., Taddei, N., van Nuland, N. A., Magherini, F., Stefani, M., Ramponi, G., and Dobson, C. M. (1998) Structural characterization of the transition state for folding of muscle acylphosphatase, *J. Mol. Biol. 283*, 893−903.
47. Munishkina, L. A., Phelan, C., Uversky, V. N., and Fink, A. L. (2003) Conformational behavior and aggregation of alpha-synuclein in organic solvents: modeling the effects of membranes, *Biochemistry 42*, 2720−2730.
48. Shibata, A., Yamamoto, M., Yamashita, T., Chiou, J. S., Kamaya, H., and Ueda, I. (1992) Biphasic effects of alcohols on the phase transition of poly(L-lysine) between alpha-helix and beta-sheet conformations, *Biochemistry 31*, 5728−5733.
49. Minor, D. L., Jr., and Kim, P. S. (1996) Context-dependent secondary structure formation of a designed protein sequence, *Nature 380*, 730−734.
50. Fersht, A. (1999) *Structure and Mechanism in Protein Science*, W. H. Freeman and Company, New York.
51. Fersht, A. R., and Sato, S. (2004) Phi-Value analysis and the nature of protein-folding transition states, *Proc. Natl. Acad. Sci. U.S.A. 101*, 7976−7981.
52. Settanni, G., Rao, F., and Caflisch, A. (2005) {Phi}-Value analysis by molecular dynamics simulations of reversible folding, *Proc. Natl. Acad. Sci. U.S.A. 102*, 628−633.
53. de los Rios, M. A., Daneshi, M., and Plaxco, K. W. (2005) Experimental investigation of the frequency and substitution dependence of negative phi-values in two-state proteins, *Biochemistry 44*, 12160−12167.
54. Raleigh, D. P., and Plaxco, K. W. (2005) The protein folding transition state: what are phi-values really telling us? *Protein Pept. Lett. 12*, 117−122.
55. Diaz, M. D., Fioroni, M., Burger, K., and Berger, S. (2002) Evidence of complete hydrophobic coating of bombesin by trifluoroethanol in aqueous solution: an NMR spectroscopic and molecular dynamics study. *Chemistry 8*, 1663−1669.
56. Fioroni, M., Diaz, M. D., Burger, K., and Berger, S. (2002) Solvation phenomena of a tetrapeptide in water/trifluoroethanol and water/ethanol mixtures: a diffusion NMR, intermolecular NOE, and molecular dynamics study. *J. Am. Chem. Soc. 124*, 7737−7744.
57. Gast, K., Siemer, A., Zirwer, D., and Damaschun, G. (2001) Fluoroalcohol-induced structural changes of proteins: some aspects of cosolvent-protein interactions, *Eur. Biophys. J. 30*, 273−283.
58. Liang, F. T., Steere, A. C., Marques, A. R., Johnson, B. J., Miller, J. N., and Philipp, M. T. (1999) Sensitive and specific serodiagnosis of Lyme disease by enzyme-linked immunosorbent assay with a peptide based on an immunodominant conserved region of *Borrelia burgdorferi* vlsE, *J. Clin. Microbiol. 37*, 3990−3996.
59. Philipp, M. T., Bowers, L. C., Fawcett, P. T., Jacobs, M. B., Liang, F. T., Marques, A. R., Mitchell, P. D., Purcell, J. E., Ratterree, M. S., and Straubinger, R. K. (2001) Antibody response to IR6, a conserved immunodominant region of the VlsE lipoprotein, wanes rapidly after antibiotic treatment of *Borrelia burgdorferi* infection in experimental animals and in humans, *J. Infect. Dis. 184*, 870−878.
60. Athanasas-Platsis, S., Somodevilla-Torres, M. J., Morton, H., and Cavanagh, A. C. (2004) Investigation of the immunocompetent cells that bind early pregnancy factor and preliminary studies of the early pregnancy factor target molecule, *Immunol. Cell Biol. 82*, 361−369.
61. Sadacharan, S. K., Cavanagh, A. C., and Gupta, R. S. (2001) Immunoelectron microscopy provides evidence for the presence of mitochondrial heat shock 10-kDa protein (chaperonin 10) in red blood cells and a variety of secretory granules, *Histochem. Cell Biol. 116*, 507−517.
62. Cappello, F., Bellafiore, M., David, S., Anzalone, R., and Zummo, G. (2003) Ten kilodalton heat shock protein (HSP10) is overexpressed during carcinogenesis of large bowel and uterine exocervix, *Cancer Lett. 196*, 35−41.
63. Slavotinek, A. M., and Biesecker, L. G. (2001) Unfolding the role of chaperones and chaperonins in human disease. *Trends Genet. 17*, 528−535.
64. Higurashi, T., Yagi, H., Mizobata, T., and Kawata, Y. (2005) Amyloid-like fibril formation of co-chaperonin GroES: nucleation and extension prefer different degrees of molecular compactness. *J. Mol. Biol. 351*, 1057−1069.

BI060464V